Bio-Inspired Hydrogen-Bond Cross-Link Strategy toward Strong and Tough Polymeric Materials

ARTICLE *in* MACROMOLECULES · JUNE 2015

Impact Factor: 5.8 · DOI: 10.1021/acs.macromol.5b00673

4 AUTHORS, INCLUDING:

Zhiguang Xu
Deakin University
24 PUBLICATIONS **435** CITATIONS
SEE PROFILE

Qipeng Guo
Deakin University
87 PUBLICATIONS **1,413** CITATIONS
SEE PROFILE

Macromolecules

Article

pubs.acs.org/Macromolecules

Bio-Inspired Hydrogen-Bond Cross-Link Strategy toward Strong and Tough Polymeric Materials

Pingan Song,[†,‡] Zhiguang Xu,[†] Yuan Lu,[§] and Qipeng Guo*[,†]

[†]Polymers Research Group, Institute for Frontier Materials, Deakin University, Locked Bag 20000, Geelong, VIC 3220, Australia

[‡]Department of Materials, College of Engineering, Zhejiang Agriculture & Forestry University, Hangzhou 311300, China

[§]Oak Ridge National Laboratory, Oak Ridge, Tennessee 37830, United States

Supporting Information

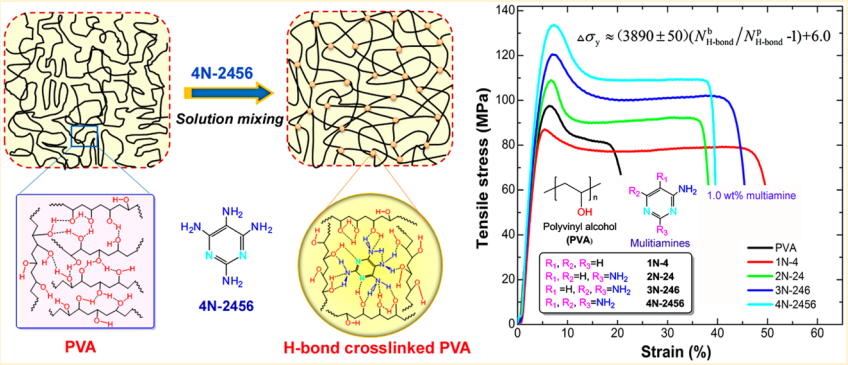

ABSTRACT: It remains a huge challenge to create advanced polymeric materials combining high strength, great toughness, and biodegradability so far. Despite enhanced strength and stiffness, biomimetic materials and polymer nanocomposites suffer notably reduced extensibility and toughness when compared to polymer bulk. Silk displays superior strength and toughness via hydrogen bonds (H-bonds) assembly, while cuticles of mussels gain high hardness and toughness via metal complexation cross-linking. Here, we propose a H-bonds cross-linking strategy that can simultaneously strikingly enhance strength, modulus, toughness, and hardness relative to polymer bulk. The H-bond cross-linked poly(vinyl alcohol) exhibits high yield strength (~140 MPa), reduced modulus (~22.5 GPa) in nanoindention tests, hardness (~0.5 GPa), and great extensibility (~40%). More importantly, there exist semiquantitive linear relationships between the number of effective H-bond and macroscale properties. This work suggests a promising methodology of designing advanced materials with exceptional mechanical by adding low amounts (≤1.0 wt %) of small molecules multiamines serving as H-bond cross-linkers.

1. INTRODUCTION

Polymeric materials have increasingly found extensive applications, spanning various fields covering construction, vehicles, electrics and electronics, and aircrafts since their discovery. However, as opposed to metal and its alloys as well as ceramic materials, most of polymers are thermally unstable and tend to deform and break at low applied stresses despite the great capability of flaw tolerance.[1] Thus, strong, tough, and lightweight polymeric materials have always been highly desirable. The past two decades have witnessed the formation of nanocomposites as one effective way to create high-performance polymer composites by adding a very low loading of nanofillers because of their distinct nanometer size effects and outstanding mechanical properties.[2−4] However, these mechanically strengthening materials usually suffer from decreased toughness to different extent relative to polymer matrices. Nature has long found its way to magically tackle this dilemma between stiffness and toughness via creating sophisticated hierarchical structures for many biological materials like bone, wood, and nacre exhibiting exceptional combination of high strength, stiffness, and toughness.[5−7]

Typical biological materials like silk, particularly spider silk, feature extraordinary strength (ultimate tensile strength of 1−2 GPa), stiffness (initial modulus of ~10 GPa), and toughness (strain at failure ≥50%) via a multiscale hierarchical structure based on mechanically inferior H-bond.[8] Recent research reveals that the highly well-organized, densely H-bonds β-sheet nanoscrystals confined to several nanometers within a ductile protein matrix synergistically resist deformation and failure to make spider silk exhibit such superior mechanical properties.[9,10] Cuticles of marine mussels have recently been discovered to be a polymeric protein scaffold stabilized by catechoto−iron chelate complexes, where the dense metal comlexation cross-linking in the granules provides high hardness while less cross-linked matrix retains good flaw

Received: March 31, 2015
Revised: May 20, 2015
Published: June 3, 2015

DOI: 10.1021/acs.macromol.5b00673
Macromolecules 2015, 48, 3957−3964

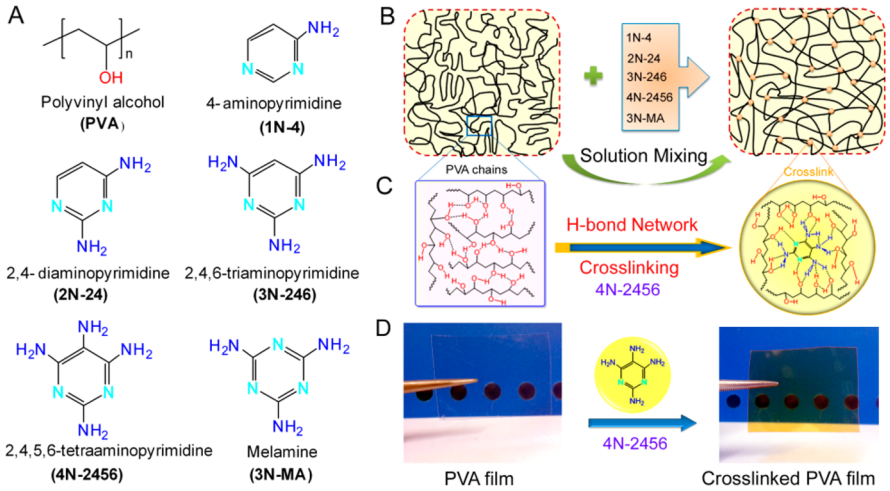

Figure 1. Fabrication H-bond cross-linked PVA and possible intermolecular interactions. (A) Chemical structures of PVA and five kinds of small molecular multiamine cross-linkers. (B) Schematic illustration of interactions for PVA and its cross-linked blends created via a simple solution mixing method. (C) Possible H-bond interactions among PVA chains and PVA with **4N-2456**. (D) Digitals images of PVA film and **4N-1.0**.

tolerance due to high stability and rates of formation.[11] Cross-linking formed by metal complexation in natural biological load-bearing structures has also been exploited as a versatile cross-linking strategy for tuning both the strength and toughness of polymeric materials like spider silks. Of interest is that incorporating some metals into inner protein structures is capable of greatly improving both of them via metal-coordination cross-links.[12,13] Therefore, nature has shown us that mechanically balanced polymeric materials can be created if one can effectively harness both H-bond and cross-linking strategy. Actually, Cordier et al. have successfully prepred supremolecular rubber via hydrogen bond assembly, and this rubber displays great self-healing and thermoreversible properties.[14]

More importantly, our preliminary attempt has shown that improved strength, stiffness, and toughness along with enhanced thermal properties can be achieved by using small amounts of melamine as H-bond cross-linker for poly(vinyl alcohol) (PVA).[15] In this work, we attempt to systematically tailor the mechanical of PVA via tuning the cross-link density of H-bond by selecting a series of pyrimidine-derived multiamines molecules and melamine as H-bond cross-linkers and uncover the relationship between H-bond cross-link and macroscale performances. The results demostrate that there exist semi-quantitive relationships between the cross-link density of H-bond and both mechanical and thermal properties.

2. EXPERIMENTAL SECTION

2.1. Materials. Raw materials including poly(vinyl alcohol) (PVA) (hydrolyzed: 99%; M_w: 89 000−98 000), 4-aminopyrimidine (**1N-4**), 2,4-diaminopyrimidine (**2N-24**), 2,4,6-triaminopyrimidine (**3N-246**), and melamine (**3N-MA**) were purchased from Sigma-Adrich, and 2,4,5,6-tetraaminopyrimidine (**4N-2456**) was bought from J&K Scientific, and all of them were used as received. Their chemical structures are shown in Figure 1A.

2.2. Sample Fabrication. 2 g of PVA powder was dissolved in 18 g of deionized water by heating to 90 °C to prepare a 10 wt % of PVA solution. A series of 10 wt % of H-bond cross-linked PVA solution were prepared by adding a certain amount of **1N-4**, **2N-24**, **3N-246**, **4N-2456**, and **3N-MA** into PVA solution. For comparison, each multiamine cross-linker was used to prepared PVA solutions with four loading levels of namely 0.5, 1.0, 2.0, and 5.0 wt %, except for **3N-MA** due to its different ring structure. The mixtures were sonicated for 30 min and then stirred for 4 h to ensure the full mixing of PVA and each multiamine cross-linker. After being cooled to the room temperature, all solutions were gently casted into a homemade glass mold followed by drying them at room temperature for 24 h and 60 °C for 12 h under reduced pressure. Transparent polymer films with thickness of about 80 μm were obtained by peeling them off for further tests. Identifications of all samples were marked according to the loading level of different cross-linkers. For instance, **2N-1.0** and **4N-5.0** respectively refer to the PVA blends containing 1.0 wt % **2N-24** and 5.0 wt % **4N-2456**, while **MA-1.0** represents the PVA blend with 1.0 wt % **3N-MA** to differentiate **3N-1.0** (PVA blend containing 1.0 wt % **3N-246**). The digital images of PVA and its cross-linked materials were taken using a digital camera.

2.3. Characterization. Infrared (IR) spectra of all multiamine molecules and polymers films were recorded on a Bruker Vetex-70 IR spectrometer (Germany) using a attenuated total reflectance (ATR) mode to obtained spectra of high resolution in the range of 500−4000 cm^{-1}. Dynamic frequency scanning for all polymer solutions was performed on a stress-controlled TA Discovery HR-3 rheometer (USA) equipped parallel plates with 40 mm in diameter. Frequency sweep tests were conducted from 10^{-2} to 10^{3} rad/s at strain amplitude of 1.0% to ensure the measurements within the linear viscoelastic region of 10%. All tests were carried out at a constant temperature of 23 ± 2 °C. It should be pointed out that viscoelastic behaviors were measured on polymer solution rather than polymer solid materials to avoid undesired changes of structure and interactions during testing temperatures above the melting point which is quite near to the degradation temperature of PVA.

All of the samples were cut into rectangular strips with a length of 30 mm and a width of 2.5 mm for tensile tests. The film tension was done using an Instron 100 N tensile tester at 22 ± 3 °C with a relative humidity of 25%, and each sample was tested at a loading rate of 5 mm/min with a gauge length of 10 mm. The calculation of tensile toughness is shown in the Supporting Information.

Nanoindention tests experiments were performed on an IBIS nanoindention system (UMIS II, Australia) with a Berkovich tip (a three-sided pyramidal diamond tip) to determine the hardness and the elastic modulus of polymer films fixed on the surface of steel stage with super glue. Sixteen indentations (a 4 by 4 array) were done in each case, and the average value was taken as the property of the composite. A stress-controlled mode was employed with a maximum load of 40 mN at load and unload rates of 1.0 mN/s with a hold time of 20 s at the peak load. The penetration depth for all samples was smaller than 2.2 μm, which is far below one-tenth of sample thickness for all samples to avoid the supporting effects of substrate. Hardness and elastic modulus were obtained by the built-in analysis software.

DOI: 10.1021/acs.macromol.5b00673
Macromolecules 2015, 48, 3957−3964

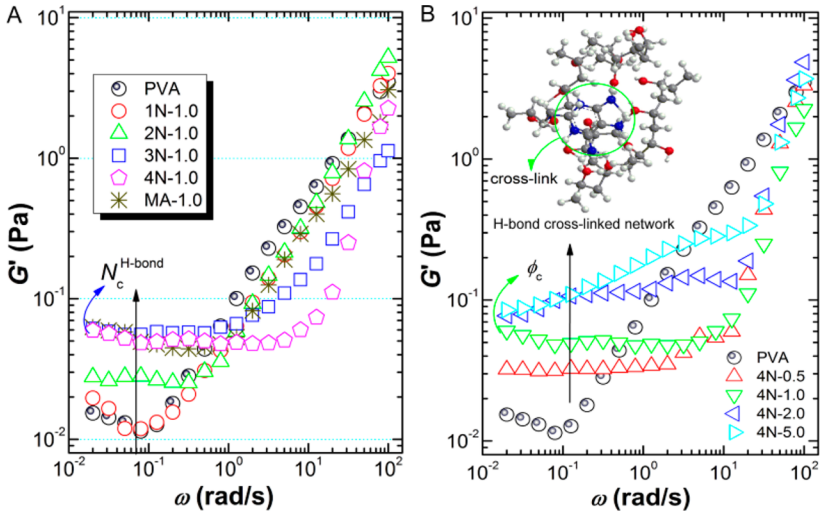

Figure 2. Frequency dependence of dynamic storage modulus (G') for (A) PVA blends with 1.0 wt % different cross-linkers and (B) PVA−**4N-2456** system as a function of loading level. All samples 10 wt % aqueous solution.

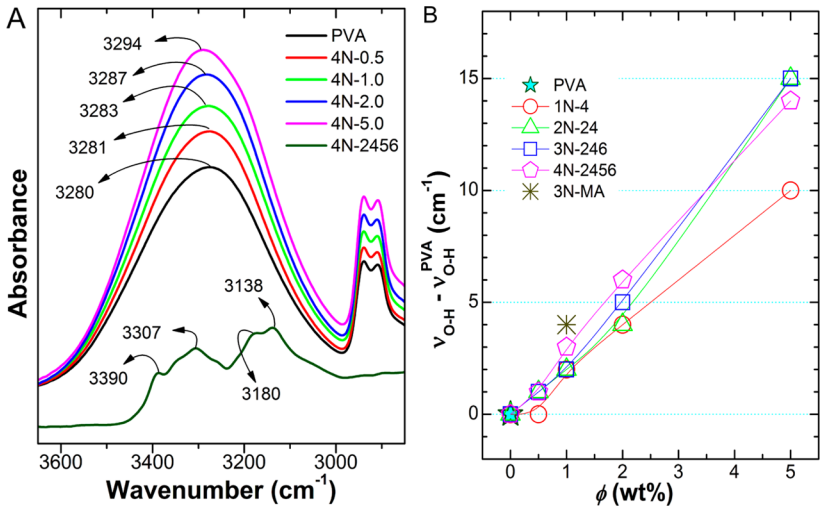

Figure 3. (A) Stretching vibrations of O−H groups (υ_{O-H}) in IR spectra for PVA, **4N-2456**, and their blends. (B) υ_{O-H} shifts of PVA cross-linked with different cross-linkers as a function of their loading level.

Dynamic mechanical analysis (DMA) tests were carried out on TA Q800 dynamic mechanical analyzer (DMA, USA). The tests temperature range was from 30 to 150 °C with a heating rate of 3 °C/min and a test frequency of 1 Hz.

Differential scanning calorimetry tests were performed on a TA Q200 differential scanning calorimeter (DSC, USA). A small amount (5−10 mg) of the sample was encapsulated in an aluminum pan and was treated with the following heat/cool/heat method under a nitrogen atmosphere. All samples were heated from 30 to 250 °C and kept at that temperature for 3 min at a scan rate of 10 °C/min (first cycle) to remove the heat history and then cooled to 30 °C at the same rate and left for 3 min (second cycle), which was then heated to 250 °C at the same heating rate (third cycle). The glass transition temperature (T_g) was obtained by taking the midpoint of two tangent lines, and the melting enthalpy was obtained by integrating the melt peak of the third cycle using the TA universal analysis software.

3. RESULTS AND DISCUSSION

3.1. Sample Preparation. All films samples are prepared via solution mixing and casting method. Figure 1B presents the schematic illustration of intermolecular interactions between PVA chains and H-bond cross-linkers, and Figure 1C demonstrates the formation of H-bond cross-linked network with **4N-2456** based on multiple H-bonds interactions, while a random H-bond network for PVA bulk. After cross-linked with 1.0 wt % of **4N-2456**, PVA film (∼100 μm thick) turns from colorless to light yellow but still transparent (Figure 1D).

3.2. Determination of Physical Cross-Linking Networks. We investigated the formation of H-bond cross-linking network in aqueous solution of PVA with different cross-linkers by rheological tests due to the high sensitivity to physical network. Apparently, the storage modulus (G') increases with increasing H-bond number or cross-linking density at low frequency (Figure 2A,B) for **2N-24**, **3N-246**, and **4N-2456** except **1N-4** because the former three types of amines can provide enough H-bond number to cross-link PVA, while **1N-4** molecules lack enough H-bond donor or acceptor (see Figure S1A−C). However, at high frequency, the G' decreases with increasing cross-linking density, primarily because the multi-amine molecule capable of form more H-bond with PVA has a larger destruction effect on the H-bond interactions among PVA chains at higher frequency, thus leading to a lower G' value.

DOI: 10.1021/acs.macromol.5b00673
Macromolecules 2015, 48, 3957−3964

In the terminal or low frequency regime, a so-called "second platform"appears once the number of effective H-bonds ($N^{\text{H-bond}}$) reaches the critical value ($N_c^{\text{H-bond}}$) for cross-linked PVA with 1.0 wt % of different multiamines (Figure 2A) or the concentration was increased to the critical concentration (ϕ_c) for **4N-2456** cross-linked PVA (Figure 2B).[16] This platform has been considered as the formation of a physical network, which will occur for cross-linkers with at least three amine groups (NH_2) each molecule at a concentration of 1.0 wt %, here only for **3N-246**, **3N-MA**, and **4N-2456**.[17,18] For **4N-2456** cross-linker, a H-bond cross-linking physical network can be created when the concentration reaches about 1.0 wt %. This suggests that PVA chains are able to be cross-linked using multiamine cross-linkers via multiple H-bonds. Additionally, the presence of multiamine cross-linkers leads to slightly smaller loss moduli (G'') relative to PVA in the whole frequency range, suggesting the reduction in visco part and the increase of elastic part of the system. Moreover, the loss factor (tan δ) peak is gradually shifted to high frequency with increasing H-bond number, clearly indicating that the relaxation of PVA segements and chains is shifted up to higher frequency due to the physical cross-link effect of multiamine cross-linkers (see Figure S3).[18]

3.3. Determination of the Number of Effective H-Bonds. IR spectra, particularly the change of stretching of hydroxyl groups (υ_{O-H}), can provide direct and powerful evidence to determine the intermolecular H-bond interactions between PVA with multiamine cross-linkers. As shown in Figure 3A, gradual blue-shifts of υ_{O-H} are clearly observed for **4N-2456** cross-linked PVA systems, e.g., from 3280 cm^{-1} for PVA to 3294 cm^{-1} for **4N-5.0**, and PVA blends cross-linked with other three cross-linkers also share similar trends (see Figure 3B). Such prominent blue-shifts clearly indicate the strong H-bond interactions between PVA and multiamines via various combinations H and N or O atoms.[15]

However, after carefully comparing IR results with the relative number of total H-bond ($N_{\text{H-bond,t}}$) (see Supporting Information), we found that the relative number of intermolecular H-bonds obtained from IR measurements is to varing extent lower than the theorectical values for five multiamines when interacting with PVA (see Figure 4). This means that only some of N and H atoms in cross-linkers molecules can form intermolecular H-bonds with O and H atoms of PVA, which is mainly due to the steric hindrance and intramolecular H-bond among the multiamine molecule. Actually, five cross-linkers in solid state tend to form intra (inter)molecular H-bonds (Supporting Information, Figure S3 and Table S1), which means that intermolecular H-bonds among cross-linkers molecules are easier to generate at high concentrations in PVA blends.

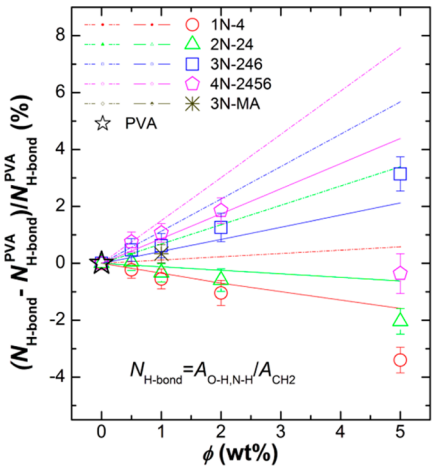

Figure 4. Comparison of relative H-bond number (hollow icons) with predicted by IR results with the number of total H-bond ($N_{\text{H-bond,t}}$, dotted lines) and the number of effective H-bond ($N_{\text{H-bond,e}}$, solid lines) for PVA blends as functions of loading level of different multiamines.

However, on the basis of IR results, we are able to calculate the number of effective H-bond for each multiamine molecule by fitting IR results and the chemical struccture of individual amultiamine molecules (see Figure 4). Interestingly, we found that for five types of multiamines (except **1N-4**), each multiamine molecule basically has about four H-bond-forming atoms like H and N atoms which do not form the intermolecular H-bond with PVA (see Supporting Information, Table S2). This probably results from the formation of intra molecular H-bonds among individual multiamine molecule. The results are well consistent with the number of effective H-bond ($N_{\text{H-bond,e}}$) predicted by IR results except at high loading level of multiamines (see Figure 4). For instance, the $N_{\text{H-bond,e}}$ (#/g) of PVA is 0.045, and **1N-4** and **2N-4** show lower $N_{\text{H-bond,e}}$ values of 0.032 and 0.036, while **3N-246**, **3N-MA**, and **4N-2456** hold higher $N_{\text{H-bond,e}}$ values of 0.056, 0.063, and 0.073, respectively (see Table S2). Therefore, we can regard adding multiamine molecules of higher $N_{\text{H-bond,e}}$ than PVA matrix as the H-bond cross-linker.

3.4. Glass Transition. The glass transition temperature (T_g) is normally considered to be the temperaure where polymer chain segments start to move. The T_g value normally increases with increasing intermolecular interactions or the presence of cross-linking, while it will decrease if intermolecular interactions become weaker or the plasticization effect exits. As expected, for PVA blends adding **1N-4** or **2N-4** leads to a linear depression with increasing loading levels because of their lower $N_{\text{H-bond,e}}$ values, while incorporating **3N-246** or **4N-2456** with higher $N_{\text{H-bond,e}}$ value increases T_g monotonously with increasing loading level ($\leq$2.0 wt %) (see Figure 5A). By fitting T_g values with the NH-bond,e, we found that the chages of T_g basically obey a simple linear relationship as functions of the relative changes of H-bond number with a coefficient (k_g) of 515 $\pm$ 8 (see Table 1). For instance, adding 1.0 wt % **4N-2456** and **1N-4** respectively display a T_g of 83.8 and 75.3 °C relative to 78.4 °C for pure PVA matrix, 2.0 wt % **4N-2456** leading to a T_g of 86.7 °C. The significant increases in T_g are primarily due to the cross-linking effects of H-bonds restricting the movements of PVA segments. However, at higher loading (>2.0 wt %) of **3N-246** or **4N-2456**, the T_g value starts to reduce significantly. For instance, adding 5 wt % of **4N-2456** almost decreases T_g down to that of PVA matrix, and this can be explained by the fact that high concentration of **4N-2456** is much easier to form small aggregates via strong intermolecular H-bond among themselves, thus leading to the plasticization effect on PVA. For **1N-4** or **2N-24** filled PVA systems, the depression of T_g is due to the weakening of H-bond network or the relative reduction of H-bond number.[15]

Meanwhile, we also investigated the effect of H-bond cross-link on the degree of crystallinity (χ_c) of PVA, as shown in Figure 5B. For five kinds of multiamines, the addition of them basically exhibits steady decreases of χ_c with increasing loading levels. For example, PVA matrix shows a χ_c of 35%, while adding 2.0 wt % of **1N-4**, **2N-24**, and **4N-2456** gives a χ_c value

DOI: 10.1021/acs.macromol.5b00673
Macromolecules 2015, 48, 3957−3964

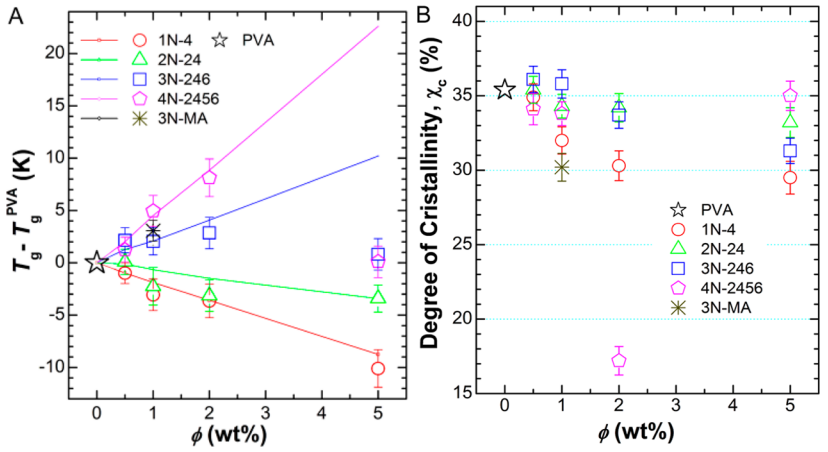

Figure 5. (A) Glass transition temperatures (T_g) changes and (B) degree of crystallinity (χ_c) of PVA with different multiamine cross-linker as functions of their weight fractions (ϕ).

Table 1. Semiquantitative Laws for Various Performances as a Function of H-Bond Number

performances	semiquantitative laws	k (k_g, k_y)
T_g (°C)	$\approx T_g^{PVA} + k_g(N^b_{H\text{-bond}}/N^p_{H\text{-bond}} - 1)$	$k_g = 515 \pm 8$
σ_y (MPa)	$\approx \sigma_y^{PVA} + k_y(N^b_{H\text{-bond}}/N^p_{H\text{-bond}} - 1 + 6.0)$	$k_y = 3890 \pm 50$

of about 30%, 34%, and 17%, respectively. The results are mainly attributed to the strong intermolecular interactions of them with PVA matrix, and the interactions may restrict the rearrangement of PVA chains during the crystallinity process. As for the sharp depression of χ_c (17%) for PVA filled 2.0 wt % **4N-2456**, probably because the criticial loading level is about 2.0 wt % for the **4N-2456** system. This means that it basically

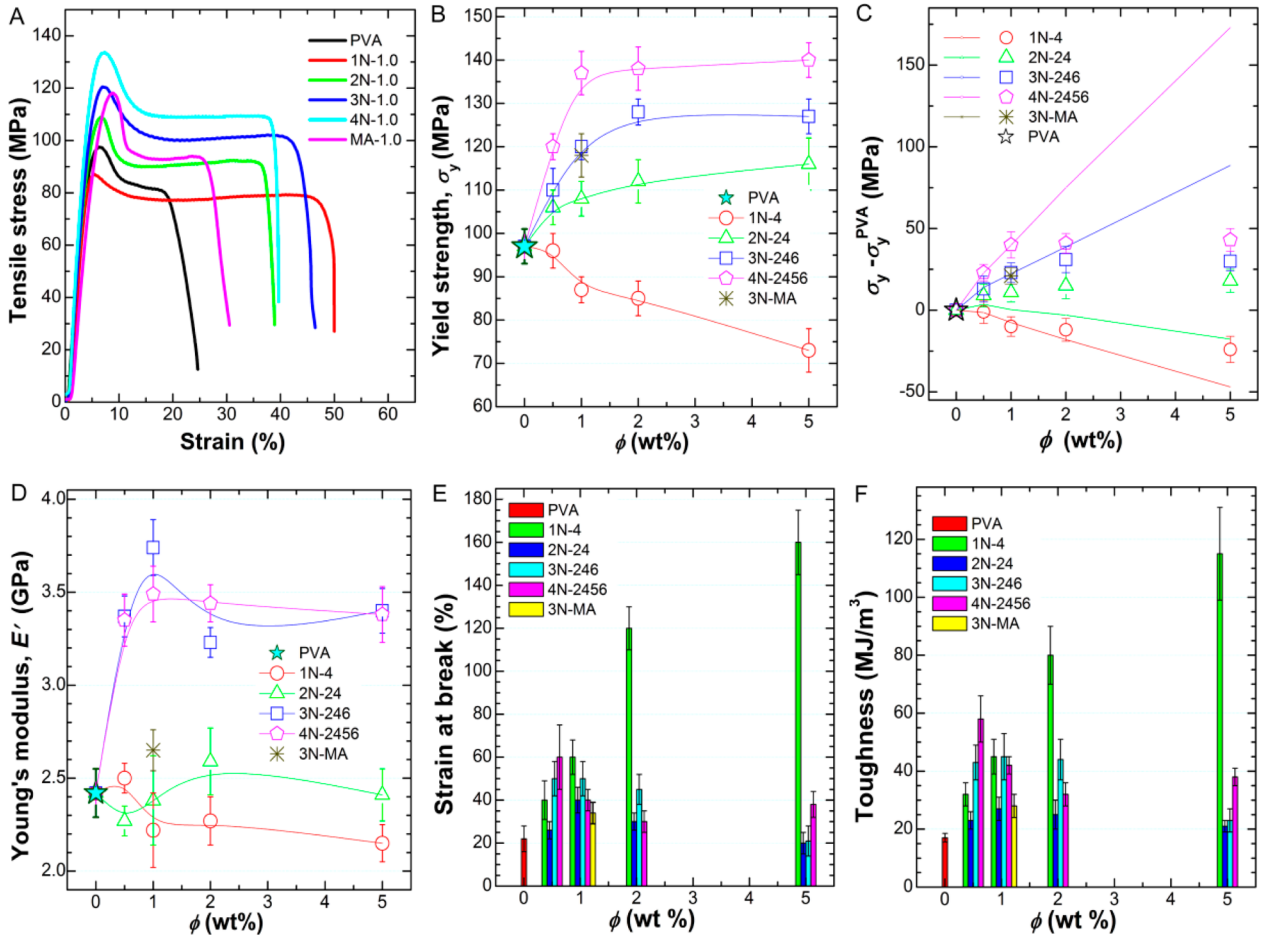

Figure 6. (A) Typical tensile stress−strain curves (loading level: 1.0 wt %), (B) yield strengths (σ_y), (D) Young's moduli (E'), (E) strain at break, and (F) tensile toughness for PVA and its blends with different multiamine cross-linkers. (C) Comparison of experimental σ_y values and the theoretical values (solid line) prediced by the relative increase in $N_{H\text{-bond,e}}$ for PVA blends.

DOI: 10.1021/acs.macromol.5b00673
Macromolecules 2015, 48, 3957−3964

forms intermolecular H-bond with PVA, thereby leading to the smallest χ_c value. However, for PVA filled with 5.0 wt % **4N-2456**, the χ_c rebounds dramatically probably because high concentration of **4N-2456** molecules readily agglomerate to form nucleation sites, thereby promoting the crystallinity.

3.5. Tensile Properties. We investigated the effect of H-bond cross-linking density on mechanical properties of PVA by controlling the concentration of H-bond cross-linkers. Figure 6A clearly shows that the tensile strength of PVA gradually increase with increasing relative H-bond density or its cross-linking density at 1.0 wt % of various multiamines accompanied by improved extensibility to different extent as compared to PVA matrix.

As shown in Figure 6B, the yield strength (σ_y) improvements are observed for PVA cross-linked by four kinds of multiamines, and these enhancements are strongly dependent on the $N_{H\text{-}bond,e}$ of multiamines, except for **1N-4** causing monotonous decrease in σ_y values due to the reduction in relative H-bond density generating the plasticization effect. Adding 1.0 wt % of **4N-2456** leads to ~43% increase in σ_y, about 138 MPa versus 97 MPa for pure PVA matrix, while 1.0 wt % of **1N-4** decreases σ_y by ~11%. Unexpectedly, **2N-24** filled PVA systems display decreased T_g values but exhibit slightly enhanced σ_y, which is proably due to different mechanisms. Additionally, σ_y changes obey the H-bond rules (Figure 6C and Table 1) for all multiamines except **2N-24** at loading levels below 5.0 wt %, since multiamines of high concentration above critical value (ϕ_c) tend to form H-bonds among themselves and generate the plasticization effect. Meanwhile, Young's moduls (E') also prominently depends on the relative changes of H-bond density, and **3N-MA**, **3N-246**, and **4N-2456** result in considerable enhancement due to the cross-linking effects while **1N-4** and **2N-24** lead to slight reduction due to the thinning effects of H-bond density (see Figure 6D). For instance, 1.0 wt % of **4N-2456**, **3N-246**, and **3N-MA** respectively exhibit enhancements by about 46% (~3.5 GPa), 54%, and 13%, and equal loading of **2N-24** displays similar E' value while **1N-4** causes slight drop by 8% in Young's modulus as compared to the PVA matrix (~2.4 GPa). The depression in both strength and stiffness caused by **14N-4** is mainly attributed to the insulation and destruction of intermolecular H-bonds in PVA, which in turn causes the plasticization effects and increased extensibility and toughness (Figure 6E,F).

Generally, strength, modulus, and toughness are normally mutually exclusive in various artificial materials,[19] while H-bond cross-linked PVA materials exhibit improved extensibility and toughness as compared to polymer matrix in the whole loading range of cross-linkers (see Figure 6E,F). 1.0 wt % of **4N-2456** displays a strain at break of about 40% and a toughness of 42 MJ m^{-3}, and 1.0 wt % of **1N-4** shows respectively 60% and 46 MJ m^{-3} as compared to 20% and 17 MJ m^{-3} for PVA matrix. Moreover, incorporating 5.0 wt % of **4N-2456** or **1N-4** still respectively leads to higher extensibility of 39% or 160% (increased by about 8-fold) despite the reduction in strength and modulus for **1N-4**. Simultaneous improvement in strength, modulus, extensibility, and toughness are unusually observed for polymeric materials reinforced with nanofillers.[2−4] Here, extensive H-bond network and particularly H-bond cross-linking (especially for **3N-246** or **4N-2456** systems) provide improved strength and stiffness due to the restriction of the unfolding of polymeric matrix. Additionally, H-bond can break under great external applied force and re-form rapidly because of the presence of abundant O and H atoms available to instantly form new H-bond once broken, since H-bond is in essence one kind of strong intermolecular interaction, not the real chemical bonds which cannot be reconstructed without external energies. This impressive feature makes H-bond cross-linked polymer materials undergo large deformation without sacrificing stiffness, enabling us to create polymers combining high strength and toughness.

When it comes to selecting materials for specific applications, the density is a major consideration. As presented in Figure 7,

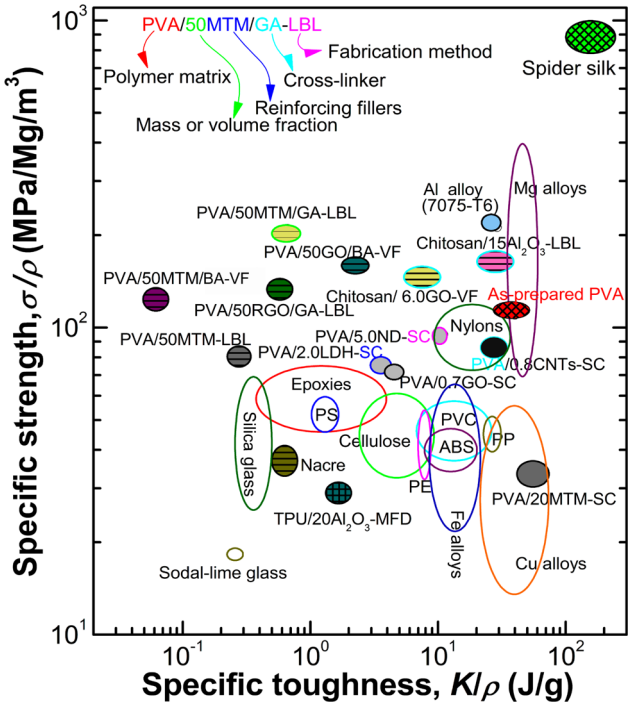

Figure 7. Diagram of specific tensile strength versus specific tensile toughness for as-prepared PVA and a range of engineering, artificial, and natural materials.[19] Detailed information for terms like PVA/50 MTM-GA/LBL and the reference are provided in Table S3 of the Supporting Information.

comparison of specific strength (σ/ρ) and specific tensile toughness (K/ρ) of a range of natural, biomimicking, and commercial polymeric materials clearly shows that **4N-2456**-cross-linked PVA materials exhibit outstanding combination of higher specific strength/toughness properties than most engineering metals and plastics such as high-performance nylons. Furthermore, as-prepared PVA materials show superior tensile toughness and comparable specific strength relative to nacre-like polymeric materials including ductile chitosan-based materials with Al_2O_3 or graphene oxides as building blocks which are mechanically anisotropic inevitably restricting their wide applications to a certain degree. Unfortunately, H-bond cross-linked PVA exhibits much lower stiffness than these mimic materials created via othe strategies, such as layer-by-layer, vacuum filtration, magnetic field driven, ice template,[20] and so on (see Figure 7 and Table S3). Additionally, H-bond cross-linked PVA is mechanically isotropic, while polymer materials prepared by traditional methods such as melt-blending and solution casting are mechanically anisotropic enabling them to apply in various fields. Compared with PVA nanocomposites reinforced with equal or slightly higher amount of nanofillers like graphene oxides and carbon nanotubes, H-bond cross-linked PVA demonstrate superior

DOI: 10.1021/acs.macromol.5b00673
Macromolecules 2015, 48, 3957−3964

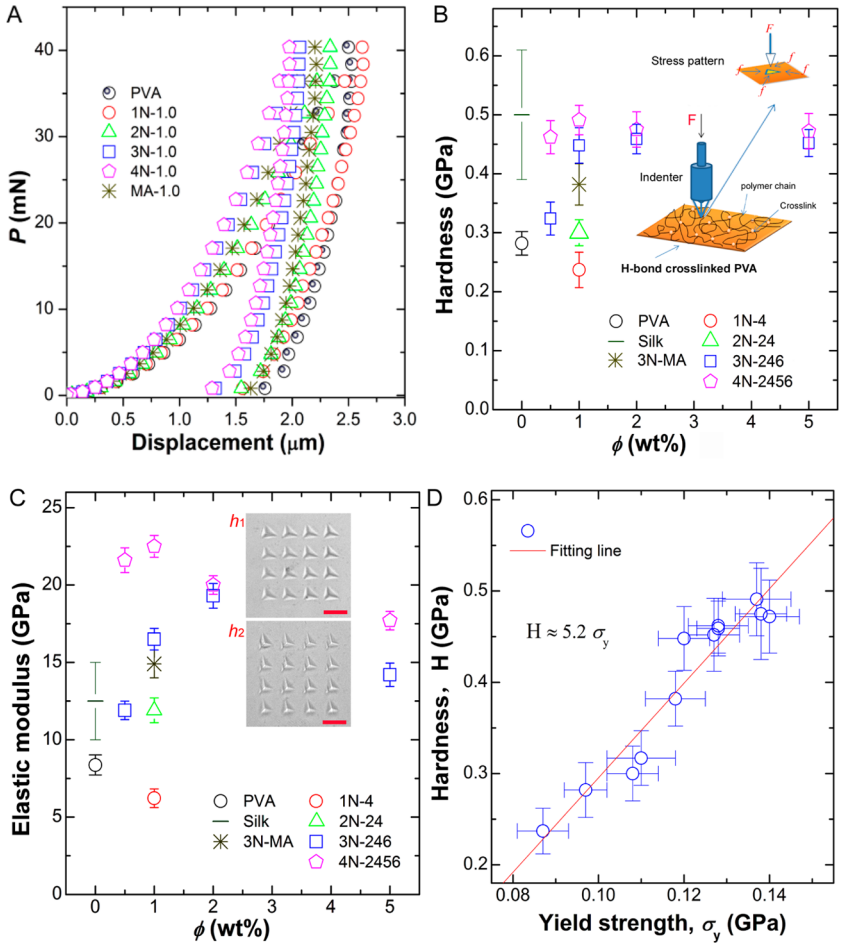

Figure 8. (A) Typical load−depth curves of PVA and its cross-linked materials with 1.0 wt % of different multiamine cross-linkers. (B) Hardness and (C) elastic moduli obtained from nanoindention tests of PVA and its cross-linked products with different cross-linker as functions of their mass fractions (ϕ). (D) Relation between hardness (H) and yield strength (σ_y) for PVA and its H-bond cross-linked materials. Inserted in (C) are microscopic nanoindentation images for PVA matrix (h_1) and 4N-1.0 (h_2), and the red scale bar is 10 μm.

strength and toughness, in spite of the higher moduli or stiffness of nanocomposites (see Figure 7 and Table S3). Therefore, though the PVA material created via H-bond cross-link strategy displays lower stiffness or moduli, it exhibits superior strength, toughness, and extensibility relative to PVA materials fabricated by other approaches.

3.6. Nanohardness. Besides traditional mechanical characterizations, nanoindention tests are also performed to examine the effect of H-bond cross-linking on the hardness and elastic modulus. Figure 8A shows typical load−depth curves of PVA and its cross-linked materials with 1.0 wt % of different multiamine cross-linkers.PVA matrix shows a hardness (H) of about 0.28 GPa while wild silk display a H of 0.4−0.6 GPa.

Obviously, the hardness changes show similar trends to yield strength changes (Figure 6B) with typical stress-control curves, as shown in Figure 8B. Addition of 1.0 wt % **4N-2456**, **3N-246**, **3N-MA**, and **2N-24** respectively result in different extent increases in hardness of 75% (0.49 GPa, falling between that of natural silk), 61% (0.45 GPa), 32% (0.37 GPa), and 11% (0.31 GPa), except slight decrease for **1N-4** (0.24 GPa). As shown in Figure 8C, reduced elastic modulus displays similar change to hardness, but the magnitudes of increase in moduli are far higher than those of hardness and Young's modulus (Figure 6D). For instance, adding 1.0 wt % of **4N-2456** or **3N-246** respectively leads to a roughly 2.75-fold (~22 GPa) or 2-fold (~16 GPa) increase in modulus as compared to pure PVA matrix (~8.0 GPa). Such great moduli are even higher than that of silk (10−15 GPa).[21] This significant enhancement in elastic modulus is primarily attributed to the confinement effects of H-bond cross-linking networks, restricting the movements and unfolding of the polymer chains. Generally, different stress patterns are mainly responsible for the different magnitudes of increase in Young's modulus from tensile tests and reduced modulus from nanoindention tests, during which the forces around the indention generate geometric confinements contributing to dramatically increased modulus.

Most importantly, we found a simple relation between hardness and yield strength, namely $H \approx 5.2\sigma_y$ (Figure 8D), slightly deviating from the Tabor's empirical relationship, $H = C\sigma_y$, where C is the constraint factor (~3.0) for fully plastic deformation.[22] This deviation is due to the fact that polymeric materials exhibit elastic and plastic deformation under tension, namely the viscoelastic behavior.

4. CONCLUSIONS

In summary, compared with assembly strategies like layer-by-layer, vacuum filtration, and ice templating, H-bond cross-linking is obviously a more time-efficient, highly effective, and scalable approach to create biodegradable polymer materials

DOI: 10.1021/acs.macromol.5b00673
Macromolecules 2015, 48, 3957−3964

with exceptional mechanical properties via a simple solution mixing and casting method without interfacial problems. Unlike nacre-biomimicking materials, H-bond cross-linked materials are mechanically isotropic. Equally importantly, H-bond cross-linking also leads to striking enhancements in the thermal stability of polymers. The H-bond cross-linking strategy developed here can be applied to many other naturally biodegradable polymers like chitosan and hydroxyethyl cellulose (Figure S6). This is extremely vital as the petrochemical-based polymers have already caused great environmental concerns like the "greenhouse effect" and also currently been facing the accelerating depletion of fossil resources.

■ ASSOCIATED CONTENT

Supporting Information

Calculation of tensile toughness and the number of H-bonds, dynamic rheological behaviors of **1N-4**, **2N-24**, and **3N-236** filled PVA solutions, ATR spectra of PVA and five kinds of multimines as well as their assignments of O−H and N−H absorption peaks, detailed description and references for various polymer composites mentioned in Figure 6, DMA results for PVA and its blends containing 1.0 wt % different multiamines, DSC curves of five kinds of multiamines, and tensile results for chitosan and hydroxyethyl cellulose filled with **4N-2456**. The Supporting Information is available free of charge on the ACS Publications website at DOI: 10.1021/acs.macromol.5b00673.

■ AUTHOR INFORMATION

Corresponding Author

*E-mail qguo@deakin.edu.au (Q.G.).

Notes

The authors declare no competing financial interest.

■ ACKNOWLEDGMENTS

P.S. was gratefully supported by an Alfred Deakin Postdoctoral Research Fellowship at Deakin University and by the National Science Foundation of China (Grant 51303162) and the Nonprofit Project of Science and Technology Agency of Zhejiang Province of China (2013C32073 and 2012C22077).

■ REFERENCES

(1) Bonderer, L. J.; Studart, A. B.; Gauckler, L. J. *Science* **2008**, *319*, 1069.
(2) Zanetti, M.; Camino, G.; Reichert, P.; Mülhaupt, R. *Macromol. Rapid Commun.* **2000**, *22*, 176.
(3) Song, P. A.; Xu, L. H.; Guo, Z. H.; Zhang, Y.; Fang, Z. P. *J. Mater. Chem.* **2008**, *18*, 5083.
(4) Potts, J. R.; Dreyer, D. R.; Bielawski, C. W.; Ruoff, R. S. *Polymer* **2011**, *52*, 5.
(5) Munch, E.; Launey, M. E.; Alsem, D. H.; Saiz, E.; Tomsia, A. P.; Ritchie, R. O. *Science* **2008**, *322*, 1516.
(6) Meyers, M. A.; Chen, P. Y.; Lin, A. Y. M.; Seki, Y. *Prog. Mater. Sci.* **2008**, *53*, 1.
(7) Aizenberg, J.; Weaver, J. C.; Thanawala, M. S.; Sundar, V. C.; Morese, D. E.; Fratzl, P. *Science* **2005**, *309*, 275.
(8) Giesa, T.; Arslan, M.; Pugno, N. M.; Buehler, M. J. *Nano Lett.* **2011**, *11*, 5038.
(9) Keten, S.; Xu, Z. P.; Ihle, B.; Buehler, M. J. *Nat. Mater.* **2010**, *9*, 359.
(10) Nova, A.; Keten, S.; Pugno, N. M.; Redaelli, A.; Buehler, M. J. *Nano Lett.* **2010**, *10*, 2626.
(11) Harrington, M. J.; Masic, A.; Holten-Andersen, N.; Waite, J. H.; Fratzl, P. *Science* **2010**, *328*, 216.
(12) Lee, S. M.; Pippel, E.; Gösele, U.; Dresbach, C.; Qin, Y.; Chandran, C. V.; Bräuniger, T.; Hause, G.; Knez, M. *Science* **2009**, *324*, 488.
(13) Pires, M. M.; Chmielewski, J. *J. Am. Chem. Soc.* **2009**, *131*, 2706.
(14) Cordier, P.; Tournilhac, F.; Soulié-Ziakovic, C.; Leibler, L. *Nature* **2008**, *451*, 977.
(15) Song, P. A.; Xu, Z. G.; Guo, Q. P. *ACS Macro Lett.* **2013**, *2*, 1100.
(16) Wu, Q.; Shangguan, Y. G.; Du, M.; Zhou, J. P.; Song, Y. H.; Zheng, Q. *J. Colloid Interface Sci.* **2009**, *339*, 236.
(17) Kashiwagi, T.; Du, F. M.; Douglas, J. F.; Winey, K. I.; Harris, R. H.; Shields, J. R. *Nat. Mater.* **2005**, *4*, 928.
(18) Du, M.; Gong, J. H.; Zheng, Q. *Polymer* **2004**, *45*, 6725.
(19) Bouville, F.; Marire, E.; Meille, S.; Van de Moortèle, B.; Stevenson, A. J.; Deville, S. *Nat. Mater.* **2014**, *13*, 508.
(20) Munch, E.; Launey, M. E.; Alsem, D. H.; Saiz, E.; Tomsia, A. P.; Ritchie, R. O. *Science* **2008**, *322*, 1516.
(21) Du, S.; Li, J. L.; Zhang, J.; Wang, X. G. *Mater. Des.* **2015**, *65*, 766.
(22) Choi, I. C.; Kim, Y. J.; Wang, Y. M.; Ramamurty, U.; Jang, J. I. *Acta Mater.* **2013**, *61*, 7313.

DOI: 10.1021/acs.macromol.5b00673
Macromolecules 2015, 48, 3957−3964